On the way to tempera grassa: unraveling the properties of emulsion-based paint binders

Côme Thillaye Du Boullay, Maguy Jaber, Maïwenn Le Denic, Floriane Gerony, Romain Bordes, Guillaume Mériguet, Anne-Laure Rollet, Philippe Walter, Laurence de Viguerie

On the way to *tempera grassa*: unraveling the properties of emulsion-based paint binders

Côme Thillaye du Boullay[a], Maguy Jaber[a], Maïwenn Le Denic[a], Floriane Gerony[a,c], Romain Bordes[b], Guillaume Mériguet[c], Anne-Laure Rollet[c], Philippe Walter[a], Laurence de Viguerie[a]*

[a] Laboratoire d'Archéologie Moléculaire et Structurale (LAMS), UMR 8220, Sorbonne Université/CNRS, 4 place Jussieu, 75005 Paris, France

[b] Department of Chemistry and Chemical Engineering, Chalmers University of Technology, Göteborg, Sweden

[c] Laboratoire de Physico-Chimie des Électrolytes et Nano-Systèmes Interfaciaux (PHENIX), UMR 8234, Sorbonne Université/CNRS, 4 place Jussieu, 75005 Paris, France

[*] Corresponding author at LAMS, UMR 8220, Sorbonne Université/CNRS, 4 place Jussieu, 75005 Paris, France. E-mail address: laurence.de_viguerie@sorbonne-universite.fr

Graphical abstract

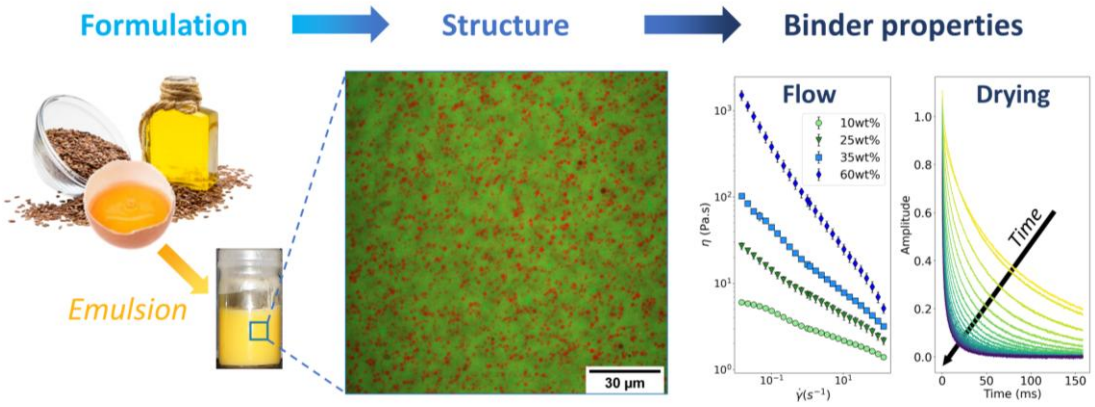

Abstract

Painting technique in Europe underwent a major change in the 15th century, when the use of egg yolk as a binder in tempera painting was gradually replaced by oil paint. This transitional period probably saw the occasional use of a mixed technique called *tempera grassa*, in which both types of binders, egg and oil, are mixed in the form of an emulsion. In order to better understand and document this historical painting practice, this article describes the physico-chemical aspects of emulsion-based binders, prepared with egg yolk and either raw linseed oil, or linseed oil partially saponified with lead oxide. Highly stable direct emulsions can be prepared with linseed oil (raw or lead-treated) and egg yolk. Remarkably, lead-treated oil also allows the formation of stable inverse emulsions. The rheological properties of direct emulsions are driven by the oil fraction: as this parameter increases from 0 to 70 wt% oil, the emulsion changes from a viscous liquid to a viscoelastic solid, which allows its flow to be easily tuned by the painter. The impact of egg yolk on the drying mechanism of the emulsion is elucidated thanks to the combined use of NMR relaxometry and FTIR spectroscopy.

Keywords

Tempera grassa, Emulsion, Rheology, Confocal microscopy, NMR relaxometry

1. Introduction

In its simplest form, paint is composed of a pigment, a colored solid powder, dispersed in a binder, a liquid phase which has the ability to dry, leading to the formation of a stiff cohesive paint film. Until the 15th century, the most widely used binder was egg yolk, in a painting technique called *a tempera*. The discovery and control of the siccative (*i.e.* 'drying') properties of vegetable oils, such as linseed or walnut oil, during the 15th century, eventually led artists to abandon egg tempera to the profit of oil paint, favored for its aesthetical advantages and longer drying times, which allowed further corrections of the works [1,2]. The evolution of painting practices during the 15th century is a topic of major interest in the field; the shift from egg tempera to oil paint probably occured as a long continuous transition rather than a sudden change. In particular, analyses of a number of European works from the 15th century revealed that both types of binders were commonly used in the same painting in different ways: in different areas of the painting [3–5], in different paint layers within the same area [6], and even mixed together in the same layer. The term *tempera grassa* is used to describe this latter painting technique, where egg yolk and oil are mixed together in a single pictorial layer. Despite a lack of historical texts from the Renaissance period describing the preparation of such a binder [1,7], the use of *tempera grassa* has been highlighted in the 1970s by staining tests carried out on cross sections from 15th century works [8]. More recently, a number of studies using chromatographic techniques coupled with mass spectrometry further supported this hypothesis [9–11], without being indisputable proof of the use of *tempera grassa* in Renaissance paintings (as these techniques do not allow the unambiguous demonstration of the co-location of oil and egg in the same paint layer). What is more certain is the use of this practice of emulsion painting in the 19th and 20th centuries by artists willing to rediscover the technique of the Renaissance *Old Masters* [12]. This revival was fostered by the writings of authors such as Max Doerner or Ralph Mayer, who published recipes of emulsion-based paints [13,14]. For instance, 20th century German painter Otto Dix was likely inspired by Doerner's recipe to develop his oil-tempera technique [15].

From a physico-chemical point of view, a binder whose major components are egg yolk and oil, is an emulsion. Indeed, the main constituent of egg yolk is water (ca. 51%), the remaining part being primarily lipids (31%) and proteins (16%) [16,17]. Previous research on egg yolk and oil emulsions have been conducted in the field of food industry, with a focus on their stability [18,19], and on the influence of parameters relevant to food applications, such as added salt or reduced cholesterol [20]. The stability of these emulsions is explained by the presence of supramolecular assemblies of egg yolk proteins and lipids, called lipoproteins. These lipoproteins adsorb on the oil/water interface and spread at the surface of oil droplets. The interfacial tension is thus lowered, stabilizing the emulsion [19,21].

Although widely studied in the field of food industry, the colloidal organization and properties of egg-oil emulsions as paint binders has been barely explored. P. Dietemann made hypotheses on the different possible colloidal systems formed in the case of *tempera grassa* [22], and investigated the effect of egg addition on an oil paint system [23], but no in-depth physico-chemical characterization has been carried on emulsion-based paint binders. It is therefore interesting to extend the research conducted by food scientists to investigate properties and materials of interest in the field of cultural heritage. In particular, we report in this study the preparation of emulsions made from egg yolk and linseed oil, commonly used by painters over centuries. Although linseed oil exhibit siccative properties, i.e. has the ability to form a solid film after a period of air exposure, this drying process, based on complex mechanism of oxidation and reticulation, is very long compared to tempera (days/weeks vs hours) where the drying process is led by evaporation of water. A very common practice was to reduce this drying time by heating the oil in the presence of lead compounds, in

particular litharge (lead oxide) as observed in numerous recipes [24]. This process results in the formation of lead soaps [25], which tend to organize at the mesoscale into structures such as liquid crystals [26,27]. Fat crystals have been reported as efficient stabilizers for o/w or w/o emulsions, in particular through Pickering mechanisms [28].

We thus studied emulsions based on egg yolk and raw linseed oil as well as lead-treated oil, to investigate how this oil treatment modifies the stability and organization of such binder, probed with confocal microscopy. Then the rheological properties of the formed emulsions were investigated, due to their particular interest for painters. Finally the drying properties of the emulsions applied as films were monitored thanks to the combination of NMR relaxometry and FTIR spectroscopy.

2. Materials and methods

2.1 Materials

Fresh organic hen eggs were purchased from a local supermarket. The egg yolk (EY) was manually separated from the white, and carefully rolled from one hand to another in order to remove all the remaining white on its surface. The vitelline membrane was punctured and the yolk collected in a beaker. To reduce the impact of variability between eggs and improve reproducibility, three egg yolks were systematically blended together manually before preparing emulsions.

Cold-pressed linseed oil (LO) from Sweden was purchased from Kremer Pigmente. The composition in fatty acids is given by the supplier as follows: 61.3% linolenic acid, 15.3% oleic acid, 14.6% linoleic acid, 4.4% palmitic acid, 2.9% stearic acid, and 1.5% others.

Lead(II) oxide PbO (>99.0%, for analysis, Emsure) was purchased from Merck. Fluorescein sodium salt (>97.5%, analytical standard, Sigma-Aldrich) and Nile Red (for microscopy, Sigma-Aldrich) were used as fluorescent dyes for confocal microscopy.

2.2 Preparation of siccativised oil with lead oxide

Lead-heated oil (LOPb) was prepared following a process described by Laporte [27], and inspired by historical recipes written by Theodore Turquet de Mayerne in 1620 [29]. 1 g of PbO was dispersed in a total of 19 g of LO at room temperature: PbO was first dispersed for 20 seconds in 2 mL of LO using a mortar and pestle. The rest of the LO was then added to the mixture, gently ground for 40 seconds and transferred into a 100 mL beaker. It was heated in a silicon oil bath at 150 °C for 2 h under magnetic stirring at 300 rpm. The final extent of the reaction was assessed by measuring the saponification rate (*i.e.* the percentage of saponified ester bonds) by FTIR-ATR (see Supplementary Fig. S1), following a protocol described in detail elsewhere [25]. Saponification rates of 15 ± 1 mol% were measured, in accordance with the results reported by Laporte [27].

2.3 Preparation of the emulsions

Emulsions were prepared with various weight fractions ϕ of LO or LOPb, ranging from 10 to 90 wt%, and defined as $\phi = m_{oil}/\left(m_{EY} + m_{oil}\right)$. A suitable amount of EY, then oil, were added in a 10 mL glass vial, for a total sample mass of 5 g. The oil was dispersed using a high-speed homogenizer (UltraTurrax T18 digital, IKA, Germany) equipped with a S18N-10G dispersing head, and operated at 15000 rpm for a total of 90 s. Every 30 s, the homogenizer was stopped to prevent the sample from heating, and the emulsion was stirred with a spatula. Emulsions were stored in the refrigerator at 5 °C.

For conductivity measurements, samples were prepared by slowly adding the oil into the EY in a mortar, while thoroughly grinding with a pestle. The slow addition of oil in this case led to an extended range of stable emulsions at high oil fractions.

For confocal microscopy, water-soluble fluorescein sodium salt was dissolved in EY. Lipophilic Nile Red was dissolved in the oil. Emulsions were then prepared using the UltraTurrax as described above.

2.4 Rheology

Rheology measurements were performed at 20 °C on a Thermo Scientific HAAKE MARS 40 rheometer, equipped with a sandblasted titanium cone and plate geometry (diameter: 35 mm, angle: 2°). A solvent hood was used to prevent water evaporation. Measurements were repeated at least twice on independently prepared samples to check reproducibility.

Dynamic properties were assessed using the following protocol:

- frequency sweep at constant strain in the linear viscoelastic regime ($\gamma = 0.1$ %) from $f = 100$ to $f = 0.01$ Hz,
- strain sweep at constant frequency ($f = 1$ Hz) from $\gamma = 0.01$ % to $\gamma = 1000$ %.

Flow measurements were carried out by increasing the shear rate from $\dot{\gamma}$ = 0.01 to 1000 s^{-1}. For shear rates lower than 1 s^{-1}, $\dot{\gamma}$ was increased by steps, each measurement point being taken when the measured stress value had reached a steady state. Between 1 s^{-1} and 1000 s^{-1}, $\dot{\gamma}$ was increased following a continuous ramp.

2.5 Confocal microscopy

Confocal microscopy was performed on a Zeiss LSM 980 upright confocal microscope. A 10x dry objective (numerical aperture: 0.3) or a 63x oil-immersion objective (numerical aperture: 1.4) were used. Fluorescein and Nile Red were excited using the 488 and 561 nm laser lines respectively, and the emitted fluorescence was collected in the 490 – 543 nm and 570 – 693 nm ranges respectively (see Supplementary Fig. S2). Images were analyzed using Fiji (ImageJ) for droplet size measurement. The average diameter was either measured manually on a large number of droplets, or using the *Particle Analysis* program of Fiji on binarized images after application of a Gaussian blur. Both methods gave similar results.

2.6 Conductimetry

Conductivity measurements were performed on a Mettler Toledo Seven Excellence conductimeter, with an InLab 731-ISM probe. A linear temperature correction was applied, so that conductivity values are reported at 25 °C.

2.7 NMR relaxometry

NMR (Nuclear Magnetic Resonance) relaxometry was carried out with the 27.63 MHz (0.65 T) NMR MOUSE PM2 (Magritek) to follow the drying of emulsions. Transverse relaxation was measured on 250 µm thick emulsion films, using a CPMG (Carr-Purcell-Meiboom-Gill) pulse sequence, with 4096 echoes separated by 38.7 µs. 90° and 180° pulses had the same duration (2.3 µs) but a 7 dB difference in the RF output power. Data were collected from a 50 µm thick region within the film. The recycle delay was 3200 ms. 1000 scans (only 75 during the first 40 min of drying) were systematically accumulated to improve signal-to-noise ratio. Data were treated using a Python code adapted from [30]: transverse relaxation signals were fitted with an inverse Laplace transform, to

compute continuous T_2 spectra [31]. The regularization parameter α for these fits was set at 0.5 (the choice of this value did not significantly impact the results).

2.8 FTIR – ATR

Changes in chemical composition during the drying of emulsions were followed using ATR – FTIR (Attenuated Total Reflexion – Fourier Transform Infrared Spectroscopy). Spectra were recorded at room temperature with a Cary 630 Agilent spectrometer equipped with the ATR module, in the 650-4000 cm^{-1} range. Small samples were regularly taken from three drying films (for reproducibility) by scratching the film with a scalpel blade. For each measurement, 64 scans were accumulated, with a spectral resolution of 4 cm^{-1}. The spectra were analyzed using OMNIC software (ThermoScientific) for integration of the band areas. Three bands were followed in particular: the OH band in the 3692-3073 cm^{-1} region (base line: 3746-3073 cm^{-1}), the C-H elongation peak in cis-HC=CH, in the 3034-2987 cm^{-1} region (base line: 3034-2987 cm^{-1}), and the C-H deformation peak in trans-HC=CH, in the 999-945cm^{-1} region (base line: 1006-945 cm^{-1}). Area values are reported without further normalization.

3. Results and discussion

3.1 Nature and stability of the emulsions

3.1.1 Emulsions with linseed oil

Emulsions with various fractions of EY and LO were prepared. When LO and EY are put together in a vial, shaken by hand as proposed by Doerner [32], the resulting emulsion is systematically highly unstable, with a visible phase separation happening in around 10 minutes (see Supplementary Fig. S3). When LO is slowly added into the EY while continuously grinding, stable emulsions can be obtained within a wide range of oil fraction, up to about 80 wt%. These emulsions, shown in Fig. 1a are stable over months when stored at 5 °C. For $\phi \geq 90\ wt\%$, phase separation happens in minutes after dispersing the LO in EY, with the latter settling at the bottom of the vial. The importance of a cautious process to prepare stable emulsions to be used as paint binders, and the deficiency of Doerner's method had already been stressed by Mayer in 1940 [14]. Indeed, the emulsification process should provide sufficient energy to generate small droplets [33]. Thus, depending on the emulsification time and intensity, emulsions of similar composition can exhibit remarkable differences in stability [34]. In this study, high shear forces are able to disrupt the oil into small droplets in emulsions formed with the mortar and pestle or with the UltraTurrax. This is not the case with emulsions prepared according to Doerner's recipe by manual shaking.

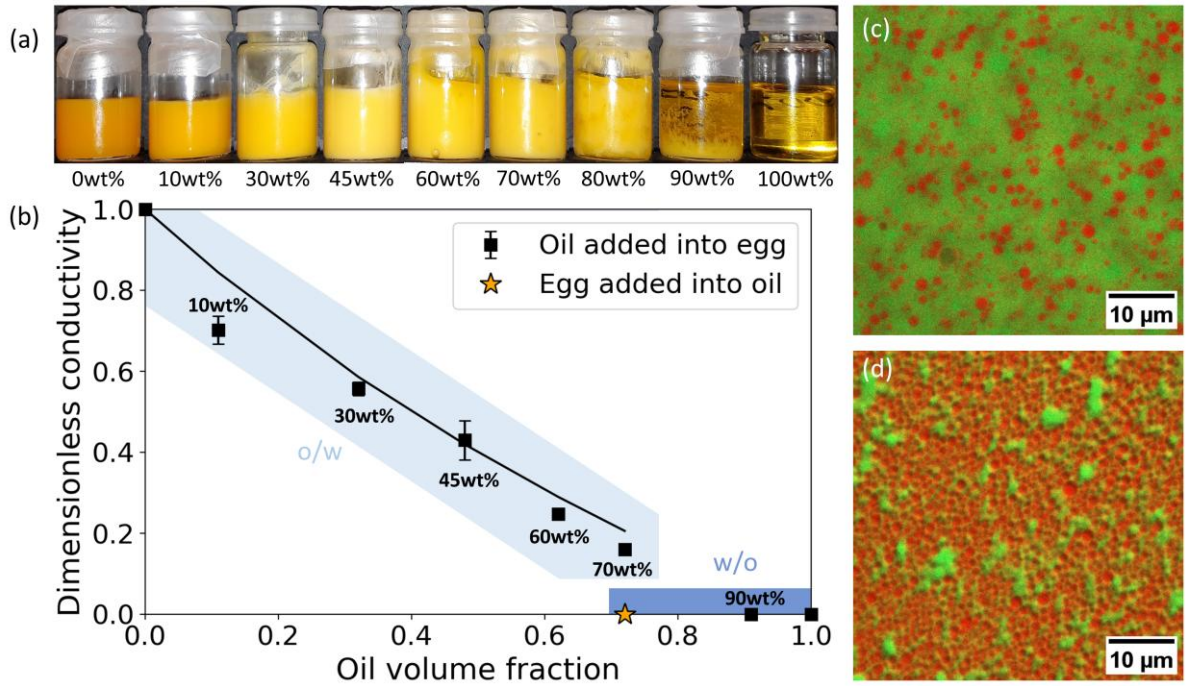

Figure 1: (a) EY + LO emulsions with various oil fractions obtained with the mortar and pestle by slowly adding LO into EY. From left to right: $\phi = 0$, 10, 30, 45, 60, 70, 80, 90 and 100 wt%. (b) Influence of the oil volume fraction on the conductivity of these emulsions (black squares). The corresponding mass fractions are given beside each point. Conductivity values are normalized by the conductivity of pure EY. Orange star: conductivity of an emulsion prepared with the mortar and pestle by slowly adding EY into LO. Black curve: Maxwell model (see eq. 1). Error bars: standard deviation from three independently prepared emulsions. (c) Confocal microscopy images (63x objective) of an emulsion with $\phi = 10\ wt\%$ and (d) $\phi = 40\ wt\%$. Water-soluble fluorescein appears in green, and oil-soluble Nile Red in red.

The nature of emulsions formed with the mortar and pestle was confirmed by conductimetry (Fig. 1b). This method has been used in the literature to track phase inversion [35]. From $\phi = 0\ wt\%$ (pure EY) to 80 wt%, emulsions have a non-zero conductivity, showing that water is the continuous phase: they are direct (o/w) emulsions. Given the high water-solubility of egg yolk lipoproteins [36], these observations are in accordance with the Bancroft rule, which states that the phase in which a surfactant has the higher solubility is the continuous phase [37]. When dividing conductivity values by the conductivity of the continuous phase (*i.e.* the conductivity of pure EY), theoretical conductivity values may be computed with a law proposed by Maxwell [38]:

$$K = \frac{k}{k_c} = \frac{1 + 2B\phi_v}{1 - B\phi_v} \qquad [1]$$

where K is the dimensionless conductivity, k the emulsion conductivity, k_c the conductivity of the continuous phase, ϕ_v the dispersed phase volume fraction, and B is defined as $B = (k_d - k_c)/(k_d + 2k_c)$, with k_d the conductivity of the dispersed phase. This theoretical model was originally developed for dilute dispersions of spheres, where the distance between particles is much larger than their diameter. However, it has been shown to accurately match experimental data on emulsions over a much wider range of oil volume fractions [39]. In our samples, $k_d \ll k_c$, so equation 1 simplifies to $K = (1 - \phi_v)/(1 + \phi_v/2)$. Experimental data shown in Fig 1.b follow

Maxwell's model reasonably well, even though the dispersed phase volume fractions computed here only take into account the oil volume, and not the dispersed components of EY, such as granules or lipoproteins.

Emulsions with $\phi > 90\ wt\%$ have a conductivity equal to zero: phase inversion happens during preparation, yielding inverse (w/o) emulsions. However, as described earlier, such emulsions are highly unstable. In order to try to promote the formation of a stable inverse emulsion, EY was slowly added into LO while thoroughly grinding with the pestle. Once again, the conductivity value for this sample is zero (star-shaped marker on Fig 1.b), but this emulsion is also highly unstable: phase separation happens in a few minutes. Thus, as exposed elsewhere [22], and in accordance with the Bancroft rule, it was not possible to obtain a stable w/o emulsion with LO and EY.

Direct imaging of emulsions can be achieved using confocal microscopy after labeling each phase with a fluorescent dye [40,41]. Such a protocol was optimized for our samples using Nile Red and fluorescein to stain the oil and aqueous phase respectively. This strategy was applied to emulsions with 10 wt% and 40 wt% LO. Pictures shown in Fig. 1c-d confirm conductimetry results: oil droplets stained with Nile Red can clearly be distinguished from the continuous aqueous phase stained with fluorescein. A median droplet diameter of 1.5 µm with a standard deviation of 0.3 µm were measured on 120 droplets from picture 1c.

3.1.2 Influence of the oil preparation: emulsions with lead-heated oil

The impact of the oil preparation on the formulation of these emulsions was further studied. As mentioned in the introduction, in order to improve the oil siccativity, numerous recipes recommend the use of lead compounds, added during heating of the oil, which leads to the partial saponification of the triglycerides in the oil. LO was thus heated with 5 wt% of lead oxide PbO in accordance with the historical recipes, resulting in saponification rates of 15 ± 1 % (see section 2.2).

Once again, using a high-speed homogenizer, stable direct emulsions can be obtained with EY and LOPb on a wide range of oil fractions. These emulsions are shown in Figure 2a. A confocal microscopy image of a direct emulsion with 50 wt% LOPb is displayed in Figure 2c. As observed previously with uncooked LO, small droplets stained with lipophilic Nile Red can be seen. The average LOPb droplet diameter is around a few hundreds of nanometers, a value significantly lower than in emulsions made with uncooked LO. Due to the small size of these droplets (of the order of magnitude of the microscope resolution), an exact diameter measurement could not be made in this case. A mixed mechanism could therefore be considered to explain the stability of these emulsions, with lipoproteins from the EY lowering the interfacial tension and facilitating the emulsion as exposed in section 3.1.1, while the lead soaps would act as an additional stabilizer.

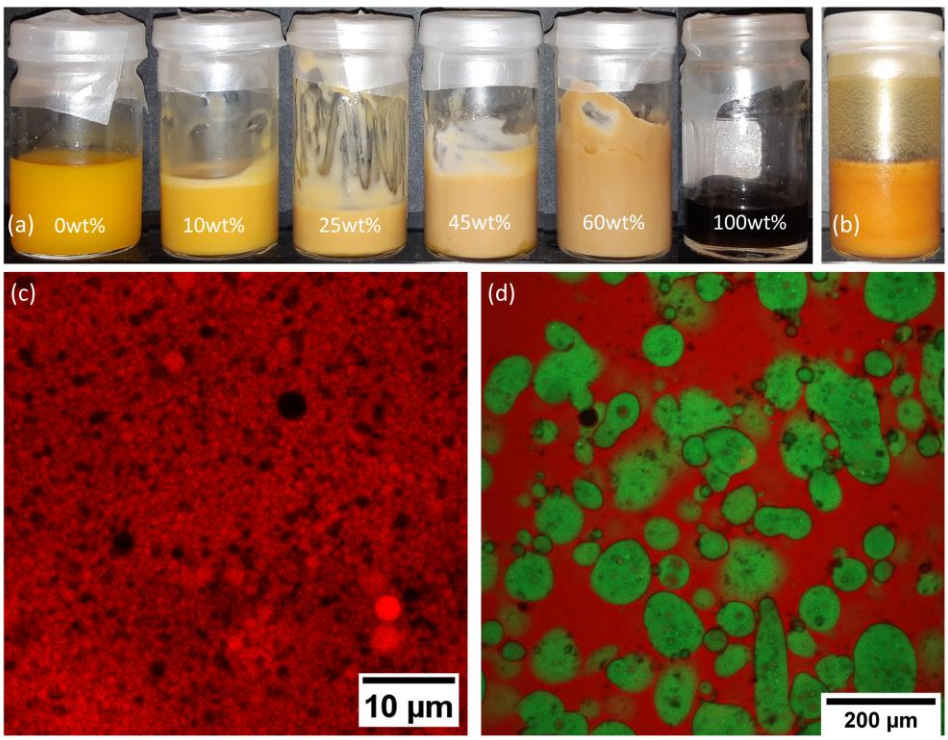

Figure 2: (a) EY and LOPb direct emulsions with various oil fractions, obtained with the UltraTurrax. From left to right: ϕ = 0, 10, 25, 45, 60, and 100 wt%. (b) EY and LOPb inverse emulsion with ϕ =50wt% oil, obtained by manually shaking the glass vial containing both phases. (c) Confocal microscopy image of a 50wt% direct emulsion obtained with the UltraTurrax (63x objective) and (d) of a 50wt% inverse emulsion obtained by manually shaking the glass vial containing both phases (10x objective). Fluorescein appears in green, and Nile Red in red. For the sake of clarity, only Nile Red is shown on picture (c)

Furthermore, emulsions were also prepared by brief vial shaking, following Doerner's process. Remarkably, emulsions stable for several days were obtained with LOPb (see Fig. 2b), in contrast to the case of LO where such process yields highly unstable emulsions (section 3.1.1). The characterization by confocal microscopy suprinsinlgy reveals the presence of large droplets of aqueous phase with characteristic sizes ranging from around 10 µm to more than 100 µm, dispersed in a continuous oil phase (Fig. 2d): w/o emulsions could be thus prepared this way for the first time. These droplets are in contact with each other but do not coalesce. The reasons for this increased stability are still uncertain, but these observations may suggest a different mechanism for the stabilization of this emulsion. Saturated lead soaps have been shown to organize into crystalline domains [26,42], with a mechanism similar to what is observed more generally with fatty acids. Fat crystals are known for their ability to stabilize o/w or w/o emulsions, with three reported mechanisms depending on their surface activity and concentration [28,43]. Fat crystals may work as Pickering stabilizers, covering the surface of the droplets and providing steric barriers against coalescence [44]. They may also form a percolating network within the continuous phase. As a result, the viscosity of this continuous phase is increased, and the diffusion of dispersed droplets is hindered. Finally, both Pickering and network mechanisms may happen simultaneously. In our samples, the oil phase is composed of saturated, mono- and polyunsaturated chains. Despite the high amount of such polyunsaturated chains, aggregates of lamellar domains in LOPb were reported by Laporte [27,45]. Further research is currently being carried out to state whether such domains are able to stabilize the emulsions or to evolve into fat crystals in the emulsions formed, which would

explain the distinctive stability of w/o emulsions prepared with LOPb compared to unstable emulsions prepared with LO.

3.2 Rheological properties

The way paint flows is a critical criterion for an artist, as it impacts not only the way it can be applied when still fresh, but also the final aspect of the paint after drying [46]. In the field of food science, rheological studies are generally limited to the domain of concentrated emulsions only, such as the mayonnaise system, due to their importance in the food industry [47,48]. Investigating the rheological properties of emulsions paint binders of different formulations over a wide range of concentrations is thus crucial to better understand the artist's gesture and choices. Rheological measurements were thus carried out on EY and LO direct emulsions.

First, flow properties are presented in Figure 3. Measurements on a wide range of shear rates are particularly relevant in the field of paint materials, as paint is subjected to shear rates as high as 1000 s^{-1} when applied with a brush, as well as very low shear rates when drying [49]. As usually observed with emulsions, the viscosity η increases with an increasing fraction of dispersed phase [50–52]. Another noticeable effect is the evolution of the dependence of η with the shear rate $\dot{\gamma}$. Emulsions with low dispersed phase fraction ($\phi = 10\ wt\%$ for instance) exhibit an almost Newtonian behavior, with a viscosity barely dependent on the shear rate. As the fraction of oil is increased, non-Newtonian effects become stronger, and emulsions display a strong shear-thinning behavior, which can be described with a power-law equation:

$$\eta = K\dot{\gamma}^{n-1} \qquad [2]$$

Experimental values obtained for K and n are given in Table 1. The flow behavior index n is smaller than 1 for all the emulsions prepared, and decreases with an increasing oil fraction in the emulsion, in line with the more pronounced shear-thinning behavior of such concentrated emulsions. This evolution may be explained by the structure of the emulsions at the colloidal scale. As mentioned in the introduction, lipoproteins in egg yolk cover the interface of the oil droplets and stabilize the emulsion. Lipoproteins adsorbed on neighboring droplets can interact with each other, leading to the formation of networks in the emulsion [47,48]. As the oil fraction increases, the average distance between neighboring droplets is reduced, allowing more interactions between the adsorbed proteins, and hence the observed evolution of rheological properties. Thanks to this strong shear-thinning, despite the high viscosity at rest (*i.e.* at low $\dot{\gamma}$ values) of concentrated emulsions, which prevents pigment sedimentation, these materials remain easily spreadable at higher shear rates, typical of paint film application.

ϕ (wt%)	K (Pa.s^n)	n
10	3.2	0.84
25	7.9	0.74
35	19	0.63
45	35	0.53
60	101	0.40

Table 1: influence of oil fraction on the flow properties of o/w emulsions. K and n measured from a power-law model as defined in equation 2.

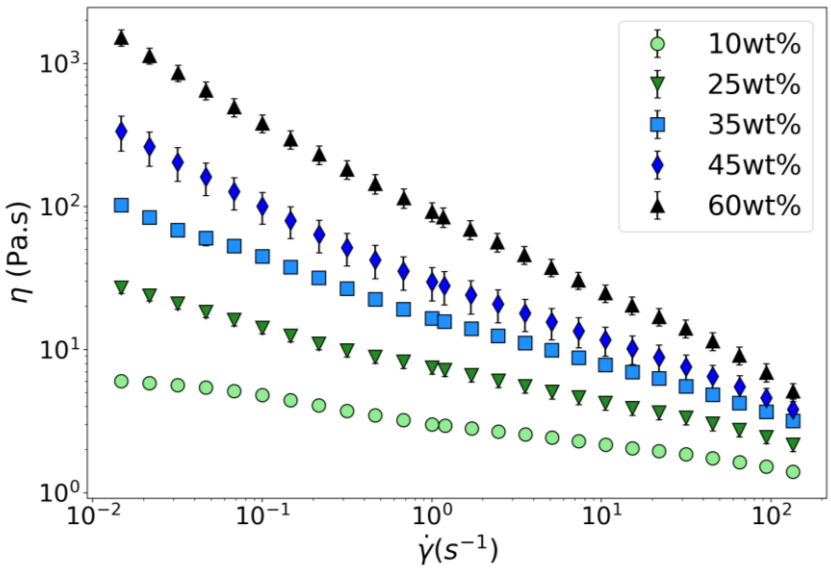

Fig 3: Effect of the oil weight fraction on the flow curves of EY and LO direct emulsions. Error bars: standard deviation for two independently prepared emulsions.

Dynamic oscillatory measurements are presented in Figure 4. In accordance with results obtained in continuous flow, the storage modulus G' and loss modulus G'' both increase with the oil fraction in the sample. Another noticeable effect is the evolution of the dependency of G' and G'' with frequency as the oil fraction is increased. Low oil fraction emulsions exhibit a liquid-like behavior with a high dependency of G' and G'' with frequency. When ϕ is increased, G' and G'' become less dependent with frequency, as would be expected from a more solid-like material. This tendency is confirmed when plotting tanδ, defined as $tan\delta = G''/G'$ (Fig 4.b). The values of tanδ strongly decrease with an increasing fraction of dispersed oil, going from $tan\delta \sim 10$ for $\phi = 10\ wt\%$, to $tan\ \delta \sim 0.1$ for $\phi = 60\ wt\%$. The inversion between G' and G'' (*i.e.* $\tan\delta = 1$) occurs when $\phi \simeq 45\ wt\%$, which is consistent with the fact that below this value, emulsions tend to flow spontaneously, whereas more concentrated samples do not exhibit this behavior. The rheological properties of o/w emulsions prepared with LOPb follow the same tendencies than those obtained with uncooked LO (see Supplementary Fig. S4).

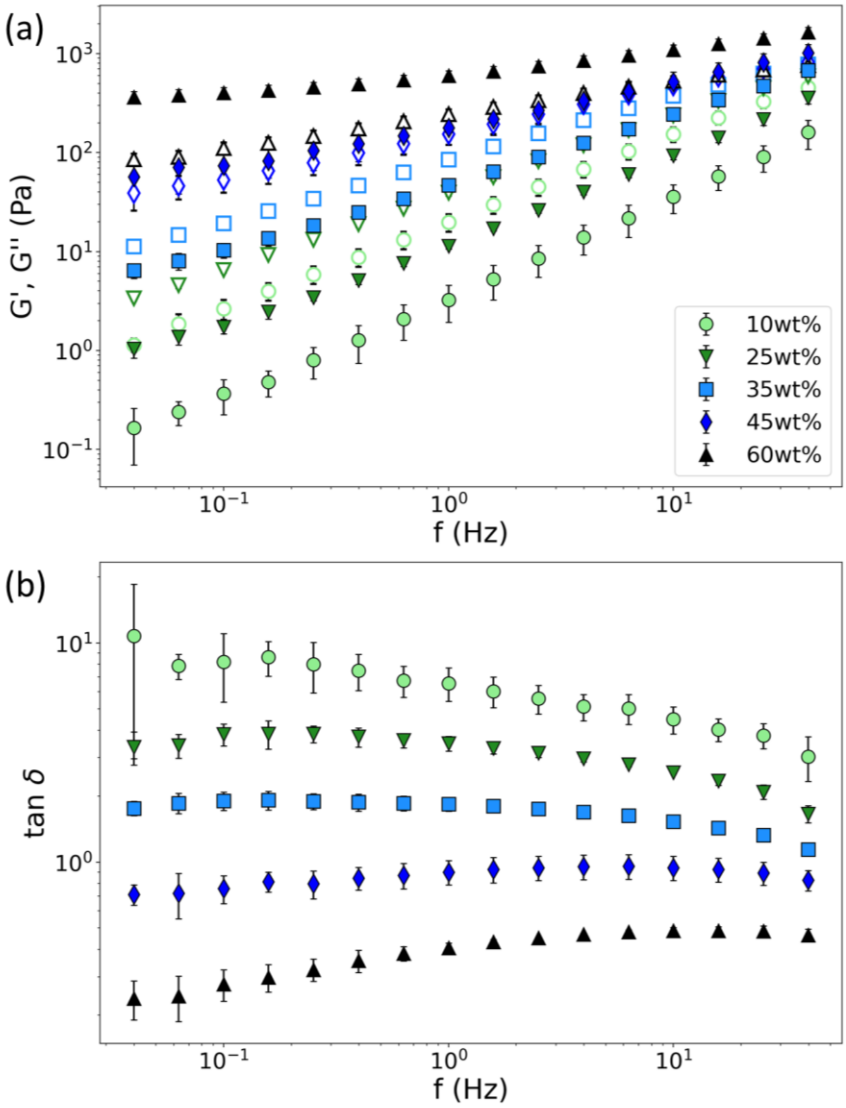

Fig 4: Dynamic rheological properties of EY and LO o/w emulsions. (a) Frequency sweep: storage modulus G' (closed symbols) and loss modulus G'' (open symbols) versus frequency for LO weight fractions ranging from 10 to 60wt%. (b) $tan\delta$ versus frequency. Error bars: standard deviation for three independently prepared emulsions.

Strain sweeps were also performed on these samples. The yield stress, defined by the intersection of the horizontal line representing the behavior of G' in the linear viscoelastic region with the power-law equation representing the behavior of G' well above the yielding point [53], was measured on emulsions with $\phi = 45\ wt\%$ and $60\ wt\%$ (see Supplementary Fig. S5). Yield stress values of ca. 5 Pa and 40 Pa were measured on emulsions with 45 wt% and 60 wt% LO respectively.

Therefore, the wide range of stable compositions allowed by the stabilizing species in EY results in various rheological properties for these emulsions. An artist preparing a paint could then easily tune the flow characteristics of its binder by changing the amount of oil added to the system.

3.3 Drying of direct emulsions

Drying properties of direct emulsions were explored. The drying of a paint binder indeed strongly influences the artistic practice. In this context, the word “drying” actually covers two different mechanisms: the drying of aqueous binders happens first through evaporation of water, whereas the drying of oil paints is the result of slower chemical processes involving the oxidation and polymerization of unsaturated oil molecules, leading to a solid crosslinked macromolecular network [54,55]. In this study the drying of o/w emulsions was followed by NMR relaxometry. Transverse nuclear magnetic relaxation happens with a time T_2 and is determined by the molecular dynamics experienced by the nuclear spins. Fast magnetic relaxation (low T_2) indicates a slow molecular mobility (rigid materials), whereas slow relaxation (high T_2) corresponds to fast molecular mobility (fluids). In order to reduce the global drying time of our samples, siccativised LOPb was used to prepare the emulsions, as it dries through similar mechanisms as LO, but in much shorter times [56]. The evolution of the relaxation of transverse magnetization during the drying of a film of emulsion is reported in Fig. 5. Two steps can be distinguished. During the first ten minutes of drying (Fig. 5a), the transverse relaxation curves quickly evolve. In the meantime, the aspect of the sample qualitatively goes from a viscoelastic material as described in section 3.2 to a solid-like film. When a biexponential function is used to measure the two main T_2 components of a fresh emulsion and of the same emulsion after 1h of drying (see Supplementary Fig. S6), the main effect observed is the strong decrease of the amplitude of the short T_2 component around 16 ms, attributed to water from the egg yolk. This first drying step thus corresponds to water evaporation from the continuous phase.

A much slower evolution follows this first step (Fig. 5b). The transverse relaxation time T_2 gradually gets shorter, until relaxation curves superimpose after about 50 h. This second step can be more accurately analyzed by plotting the evolution of the spectrum of transverse relaxation times during the drying process. The numerical inverse Laplace transform of transverse relaxation curves measured every hour after the end of the first step of drying was computed and is reported in Fig. 6. During the first ten hours of the second stage of drying, the major T_2 component is around 100 ms. This value decreases over 30 h to 10 ms. Meanwhile, shorter components appear at 5 ms, 1 ms and 0.25 ms. The latter becomes the major component after 30 hours of drying and corresponds to the very fast drop observed on the final relaxation curves (dark blue lines in Fig. 5b). This evolution towards shorter T_2 is typical of the formation of a solid material by cross-linking [31] and attributed by Busse *et al.* to the polymerization of the oil molecules [57].

Based on these observations, the drying of the emulsion can be modelled by a two-step mechanism: a first step with a characteristic timescale of 10 minutes corresponding to water evaporation, followed by the shortening of transverse relaxation times due to the cross-linking of unsaturated oil molecules.

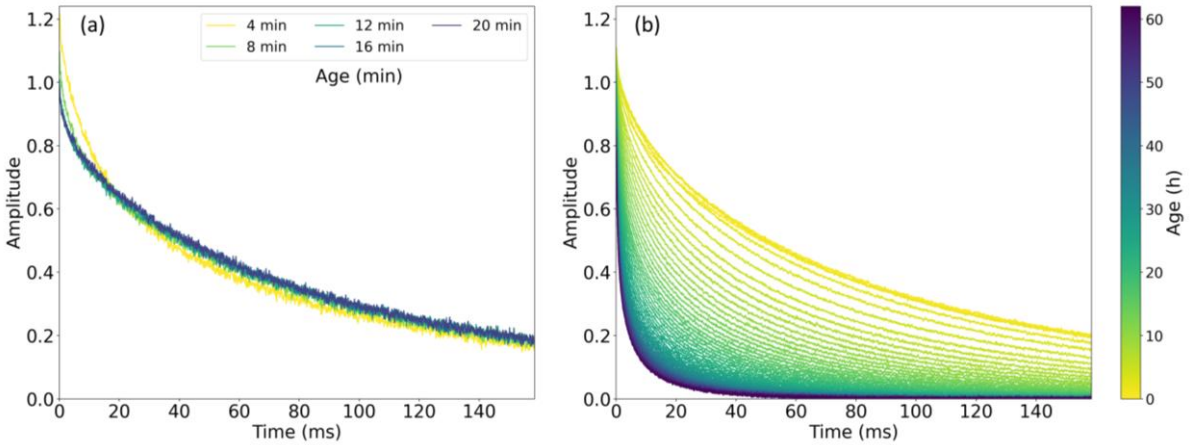

Figure 5: Evolution of the relaxation of transverse magnetization during the drying of a 250µm thick film of an o/w emulsion with $\phi = 40wt\%$ LOPb, (a) at short timescale and (b) at long timescale. For the sake of clarity in representation, data are smoothed via a running average over 10 points.

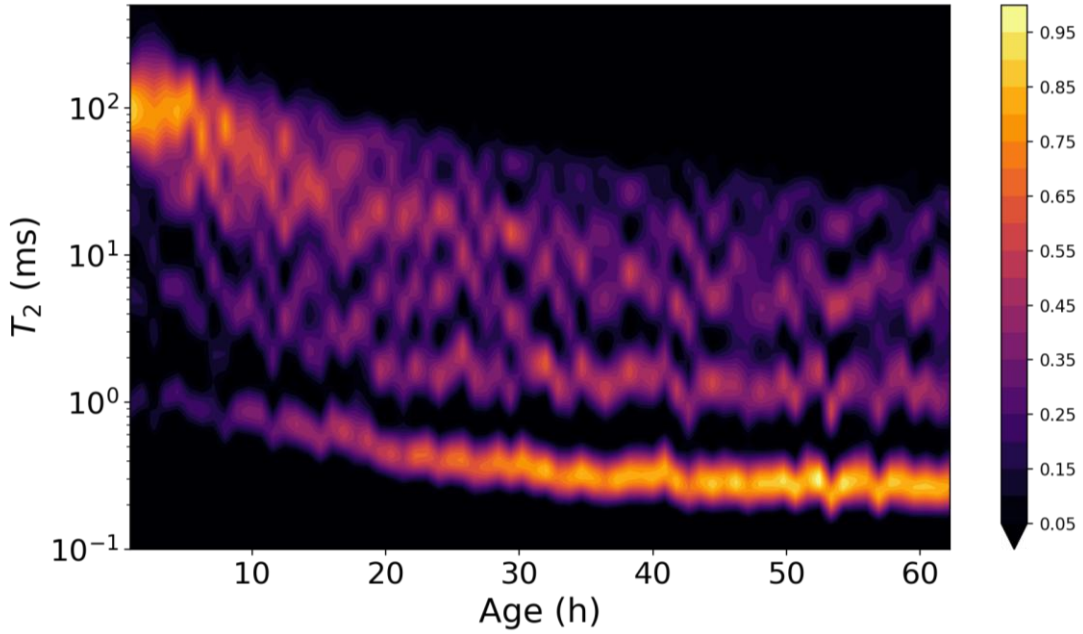

Figure 6: Evolution of the T_2 spectrum of a drying 250 µm thick film of a direct emulsion with $\phi = 40wt\%$ LOPb, during the second stage of drying. Color values : normalized T_2 amplitudes computed using the numerical inverse Laplace transform of relaxation data displayed in Fig. 5b..

To further understand the molecular mechanisms involved in the drying of emulsion films, FTIR-ATR measurements were carried out (see Fig. 7a), as previously used in the literature to monitor the drying of linseed oil films [56]. The OH band around 3350 cm^{-1}, initially very strong due to the high water content in EY, quickly fades. Its area is reduced by 80 % in 10 min before reaching a plateau (Fig. 7b). This first step can be assigned to the evaporation of water and is consistent with the NMR relaxometry results. The second step displays evolutions of peaks typically expected for the drying of a siccative oil. This step was thus assessed by following the evolution of two peaks commonly used as markers of the oxidation and cross-linking processes in siccative oils [56]: the band centered around 3010 cm^{-1}, attributed to C–H elongation in cis-HC=HC, and the band centered around 968 cm^{-1}, attributed to C–H deformation in trans-HC=HC (Fig. 7c). The simultaneous decrease of the 3010 cm^{-1} band and increase of the 968 cm^{-1} band over about 100 h is a marker of the isomerization process,

typically observed among molecular transformations during the drying of siccative oils: starting from unconjugated *cis-cis* molecules, this reaction produces more thermodynamically favorable conjugated *cis-trans* or *trans-trans* species [54]. The crosslinking of the triglycerides highlighted by FTIR is in good agreement with the evolution of the T_2 reported earlier with NMR relaxometry.

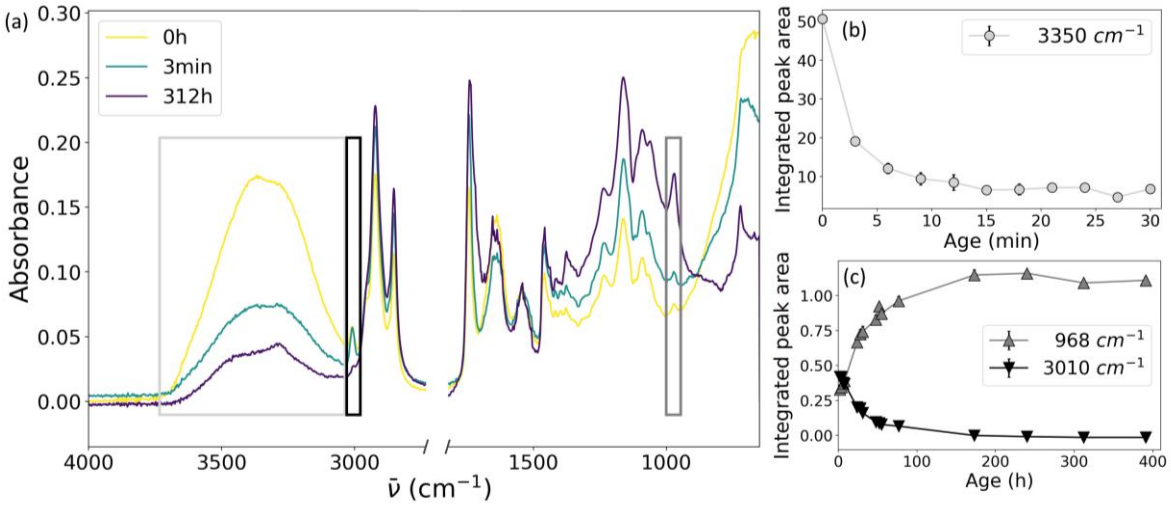

Figure 7: FTIR-ATR spectroscopy of drying direct emulsions with $\phi = 40wt\%$ LOPb. (a) Evolution of FTIR spectra during the drying of a 250µm thick film (b) Evolution of the OH band area in the 3692-3073cm^{-1} region (base line: 3746-3073 cm^{-1}) over 30min (c) Evolution of the C-H elongation peak in cis-HC=CH, in the 3034-2987 cm^{-1} region (base line: 3034-2987 cm^{-1}) and of the C-H deformation peak in trans-HC=CH, in the 999-945cm^{-1} region (base line: 1006-945 cm^{-1}), over 400h. Error bars: standard deviation on three different films.

Thus, the drying of an emulsion-based binder actually covers both aspects of drying discussed earlier: a first physical process of evaporation of water happening in minutes after spreading of a film, followed by a slower chemical process of oxidation and reticulation of the oil molecules, happening in tens of hours in the case of siccativised oils used here.

The drying kinetics of LOPb and of an emulsion with 60 wt% EY and 40 wt% LOPb were compared to assess the impact of the presence of EY on the drying of oil. The evolution of the 968 cm^{-1} band of these two materials is displayed in Fig. 8. Without added EY, the 968 cm^{-1} band area reaches a plateau after about 20 h. When oil is dispersed in EY as an emulsion, the cis-trans isomerization processes described earlier are considerably slowed down, with a plateau starting after more than 100 h. Egg yolk contains a variety of substances known for their antioxidant activity, such as phosvitin, phospholipids, carotenoids, vitamin E and aromatic amino-acids [58]. The ability of these species to scavenge free radicals formed during the auto-oxidation of unsaturated fatty acid chains may explain the slowdown of the isomerization process observed here. In the context of an artistic practice, this effect could have an impact on the ability of the painter to apply successive layers of paint. As described earlier, the first step of drying quickly yields a solid-like, dry-to-the-touch film. Therefore, as expected with a *tempera* paint, it would not be possible for an artist to use a "wet-in-wet" technique to apply successive layers of an emulsion-based paint. Conversely it allows the painter to superimpose layers without having to wait a considerable amount of time, required in the case of oil binder. However, as proved with these experiments, the oil remains liquid for a very long time after evaporation of the water. This slowed-down drying could therefore still enable a certain

degree of fusion between successive layers, which would have a definitive impact on the final aspect and on the conservation of a painting. Further tests are being conducted to assess this point.

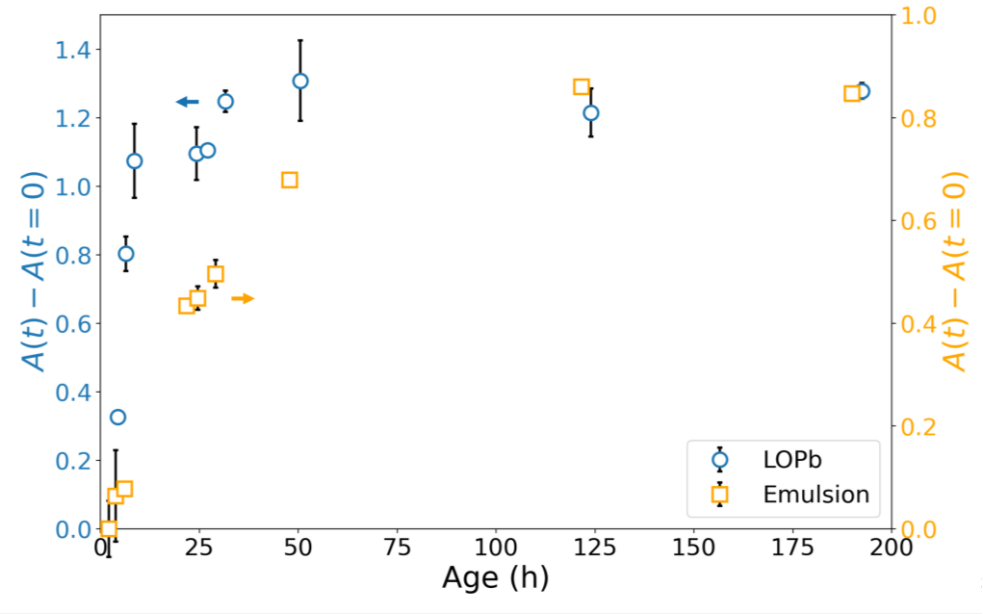

Figure 8: Impact of the presence of EY on the drying kinetics of oil: evolution of the C – H deformation peak in trans-HC=CH, in the 999-945cm^{-1} region (base line: 1006-945 cm^{-1}), over 200h, for LOPb (blue circles, left axis), and a direct emulsion with $\phi = 40wt\%$ LOPb (yellow squares, right axis). Error bars: standard deviation on three different films, 250µm in thickness.

4. Conclusion

In this work, we explored the physico-chemical properties of egg yolk and linseed oil emulsions to shed new light on their potential use as a paint binder in the *tempera grassa* painting technique, and focused on both preparation and drying of such systems. Direct (o/w) stable emulsions were prepared with a wide range of oil fractions, associated with various rheological properties, from viscous liquids to gel-like behaviors. In particular, emulsions with high oil fractions exhibit high viscosities at rest and a yield stress, but remain easily spreadable thanks to their pronounced shear-thinning. Stable reverse (w/o) emulsions could not be obtained with uncooked linseed oil. Conversely, partial saponification of the oil triglycerides with lead oxide allowed the formation of both o/w and w/o emulsions, as confirmed by confocal microscopy observations. Further research will be carried out to better understand the mechanisms at stake here. In particular, in the case of o/w emulsions, the role of the surface active properties of the lead carboxylates in the presence of egg yolk lipoproteins should be explored. In the case of w/o emulsions, research will focus on a possible Pickering mechanism, allowed by the presence of structures similar to fat crystals described in the literature as stabilizers for such emulsions [27]. Such mechanisms has been proven effective in stabilizing reverse system right in the field of food and hydrocolloids [43]. The possibility of stabilizing w/o emulsions by partially saponified oil also opens new perspectives in the cultural heritage field and raises numerous questions about their specific properties as a paint binder.

NMR relaxometry combined with FTIR analyses demonstrated a two-step drying mechanism of direct emulsions: a first step related to the evaporation of water, followed by the curing of the oil. This second step was shown to be slowed down by the presence of egg yolk, with potential impact on the painting practice and the visual aspect of the paint. Further studies are now planned to investigate the properties and advantages of paint (*i.e.* pigment-binder) systems based on such emulsions to

better understand how their peculiar properties influence the characteristics of the paint itself and may have led artists to adopt this painting technique.

CRediT authorship contribution statement

Côme Thillaye du Boullay: Conceptualization, Investigation, Validation, Formal analysis, Writing – Original draft. **Maguy Jaber:** Conceptualization, Writing – Review & Editing, Supervision. **Maïwenn le Denic:** Investigation. **Floriane Gerony:** Writing – Review & Editing. **Guillaume Mériguet:** Writing – Review & Editing. **Romain Bordes:** Writing – Review & Editing . **Anne-Laure Rollet:** Writing – Review & Editing. **Philippe Walter:** Writing – Review & Editing. **Laurence de Viguerie:** Conceptualization, Writing – Review & Editing, Supervision.

Data availability

Data will be made available upon request

Declaration of Competing Interest

The authors declare that they have no known competing financial interests or personal relationships that could have appeared to influence the work reported in this paper.

Acknowledgements

This project was funded by Sorbonne-Université – ED397. Image acquisition was performed at the IBPS Imaging Facility. The IBPS Imaging facility is supported by Region-Île-de-France, Sorbonne-University and CNRS.

References

[1] J. Dunkerton, Modifications to traditional egg tempera techniques in fifteenth-century Italy, in: Maastricht, 1996. https://www.bcin.ca/bcin/detail.app?lang=en&id=171893&asq=&csq=&csa=&ps=50&pId=1&.
[2] P. Walter, L. de Viguerie, Materials science challenges in paintings, Nat. Mater. 17 (2018) 106–109. https://doi.org/10.1038/nmat5070.
[3] R. WHITE, J. PILC, Analyses of Paint Media, Natl. Gallery Tech. Bull. 17 (1996) 91–103.
[4] C. Higgitt, R. White, Analyses of Paint Media: New Studies of Italian Paintings of the Fifteenth and Sixteenth Centuries, Natl. Gallery Tech. Bull. 26 (2005).
[5] L. de Viguerie, N.O. Pladevall, H. Lotz, V. Freni, N. Fauquet, M. Mestre, P. Walter, M. Verdaguer, Mapping pigments and binders in 15th century Gothic works of art using a combination of visible and near infrared hyperspectral imaging, Microchem. J. 155 (2020) 104674. https://doi.org/10.1016/j.microc.2020.104674.
[6] M. Christine Gay, Application de la méthode des colorations sur coupes minces à l'étude des liants de quelques peintures italiennes du 14e et 15e siècles, Stud. Conserv. 17 (1972) 705–713. https://doi.org/10.1179/sic.1972.17.s1.013.
[7] K. DeGhetaldi, From egg to oil: the early development of oil painting during the Quattrocento, Thesis, University of Delaware, 2016. https://udspace.udel.edu/handle/19716/23610 (accessed November 2, 2021).
[8] E. Martin, Some improvements in techniques of analysis of paint media, Stud. Conserv. 22 (1977) 63–67. https://doi.org/10.1179/sic.1977.009.
[9] C. Tokarski, E. Martin, C. Rolando, C. Cren-Olivé, Identification of Proteins in Renaissance Paintings by Proteomics, Anal. Chem. 78 (2006) 1494–1502. https://doi.org/10.1021/ac051181w.

[10] K.B. Kalinina, I. Bonaduce, M.P. Colombini, Irina.S. Artemieva, An analytical investigation of the painting technique of Italian Renaissance master Lorenzo Lotto, J. Cult. Herit. 13 (2012) 259–274. https://doi.org/10.1016/j.culher.2011.11.005.
[11] E. Barberis, M. Manfredi, E. Marengo, G. Zilberstein, S. Zilberstein, A. Kossolapov, P.G. Righetti, Leonardo's Donna Nuda unveiled, J. Proteomics. 207 (2019) 103450. https://doi.org/10.1016/j.jprot.2019.103450.
[12] L. Mayer, G. Myers, Old Master Recipes in the 1920s, 1930s, and 1940s: Curry, Marsh, Doerner, and Maroger, J. Am. Inst. Conserv. 41 (2002) 21–42. https://doi.org/10.2307/3179895.
[13] M. Doerner, Malmaterial und seine Verwendung im Bilde, Munich, Germany, 1921.
[14] R. Mayer, The Artist's Handbook of Materials and Techniques, London, 1940.
[15] B.F. Miller, Otto Dix and His Oil-Tempera Technique, Bull. Clevel. Mus. Art. 74 (1987) 332–355.
[16] M. Anton, Composition and Structure of Hen Egg Yolk, in: R. Huopalahti, R. López-Fandiño, M. Anton, R. Schade (Eds.), Bioact. Egg Compd., Springer Berlin Heidelberg, Berlin, Heidelberg, 2007: pp. 1–6. https://doi.org/10.1007/978-3-540-37885-3_1.
[17] Y. Mine, Emulsifying characterization of hens egg yolk proteins in oil-in-water emulsions, Food Hydrocoll. 12 (1998) 409–415. https://doi.org/10.1016/S0268-005X(98)00054-X.
[18] V. Kiosseoglou, Egg yolk protein gels and emulsions, Curr. Opin. Colloid Interface Sci. 8 (2003) 365–370. https://doi.org/10.1016/S1359-0294(03)00094-3.
[19] M. Anton, Egg yolk: structures, functionalities and processes, J. Sci. Food Agric. 93 (2013) 2871–2880. https://doi.org/10.1002/jsfa.6247.
[20] A. Wang, Z. Xiao, J. Wang, G. Li, L. Wang, Fabrication and characterization of emulsion stabilized by table egg-yolk granules at different pH levels, J. Sci. Food Agric. 100 (2020) 1470–1478. https://doi.org/10.1002/jsfa.10154.
[21] V.D. Kiosseoglou, P. Sherman, Influence of egg yolk lipoproteins on the rheology and stability of O/W emulsions and mayonnaise 2. Interfacial tension -time behaviour of egg yolk lipoprotein at the groundnut oil-water interface, Colloid Polym. Sci. 261 (1983) 502–507. https://doi.org/10.1007/BF01419834.
[22] P. Dietemann, A colloidal description of tempera and oil paints, based on a case study of Arnold Böcklin's painting Villa am Meer II (1865), (2014) 18.
[23] O. Ranquet, C. Duce, E. Bramanti, P. Dietemann, I. Bonaduce, N. Willenbacher, A holistic view on the role of egg yolk in Old Masters' oil paints, Nat. Commun. 14 (2023) 1534. https://doi.org/10.1038/s41467-023-36859-5.
[24] S. Zumbühl, C. Zindel, Historical siccatives for oil paint and varnishes, (n.d.).
[25] M. Cotte, E. Checroun, J. Susini, P. Dumas, P. Tchoreloff, M. Besnard, Ph. Walter, Kinetics of oil saponification by lead salts in ancient preparations of pharmaceutical lead plasters and painting lead mediums, Talanta. 70 (2006) 1136–1142. https://doi.org/10.1016/j.talanta.2006.03.007.
[26] F.J. Martínez-Casado, M. Ramos-Riesco, J.A. Rodríguez-Cheda, M.I. Redondo-Yélamos, L. Garrido, A. Fernández-Martínez, J. García-Barriocanal, I. da Silva, M. Durán-Olivencia, A. Poulain, Lead-soaps: crystal structures, polymorphism, and solid and liquid mesophases, Phys. Chem. Chem. Phys. 19 (2017) 17009–17018. https://doi.org/10.1039/C7CP02351K.
[27] L. Laporte, G. Ducouret, F. Gobeaux, A. Lesaine, C. Hotton, T. Bizien, L. Michot, L. de Viguerie, Rheo-SAXS characterization of lead-treated oils: Understanding the influence of lead driers on artistic oil paint's flow properties, J. Colloid Interface Sci. 633 (2023) 566–574. https://doi.org/10.1016/j.jcis.2022.11.089.
[28] S. Ghosh, T. Tran, D. Rousseau, Comparison of Pickering and Network Stabilization in Water-in-Oil Emulsions, Langmuir. 27 (2011) 6589–6597. https://doi.org/10.1021/la200065y.
[29] M. Faidutti, C. Versini, Le Manuscrit de Turquet de Mayenne présenté par M. Faidutti et C. Versini, Pictoria Sculptoria et quae subalternarum artium - 1620, Audin Imprimeurs, Lyon, 1967.
[30] Z. Cai, Inverse Laplace Transform of Real-valued Relaxation Data by a Regularized Non-negative Least Squares Method, 2019. https://github.com/caizkun/pyilt.
[31] B. Blümich, S. Haber-Pohlmeier, W. Zia, Compact NMR, fig.5.1.3, p.131, De Gruyter, 2014. https://doi.org/10.1515/9783110266719.

[32] M. Doerner, The Materials of the Artist and their Use in Painting - With Notes on the Techniques of the Old Masters, Hart Davis, MacGibbon, London, 1934.
[33] D.J. McClements, S.M. Jafari, Improving emulsion formation, stability and performance using mixed emulsifiers: A review, Adv. Colloid Interface Sci. 251 (2018) 55–79. https://doi.org/10.1016/j.cis.2017.12.001.
[34] E. Tornberg, A.-M. Hermansson, Functional Characterization of Protein Stabilized Emulsions: Effect of Processing, J. Food Sci. 42 (1977) 468–472. https://doi.org/10.1111/j.1365-2621.1977.tb01524.x.
[35] J. Allouche, E. Tyrode, V. Sadtler, L. Choplin, J.-L. Salager, Simultaneous Conductivity and Viscosity Measurements as a Technique To Track Emulsion Inversion by the Phase-Inversion-Temperature Method, Langmuir. 20 (2004) 2134–2140. https://doi.org/10.1021/la035334r.
[36] M. Anton, G. Gandemer, Composition, Solubility and Emulsifying Properties of Granules and Plasma of Egg Yolk, J. Food Sci. 62 (1997) 484–487. https://doi.org/10.1111/j.1365-2621.1997.tb04411.x.
[37] W.D. Bancroft, The Theory of Emulsification, V, J. Phys. Chem. 17 (1913) 501–519. https://doi.org/10.1021/j150141a002.
[38] J.C. Maxwell, A treatise on Electricity and Magnetism, Part II, Chapter IX, Clarendon Press Series, London, 1873.
[39] K.-H. Lira, D.H. Smith, Electrical conductivities of concentrated emulsions and their fit by conductivity models, J. Dispers. Sci. Technol. 11 (1990) 529–545. https://doi.org/10.1080/01932699008943276.
[40] L. Besnard, M. Protat, F. Malloggi, J. Daillant, F. Cousin, N. Pantoustier, P. Guenoun, P. Perrin, Breaking of the Bancroft rule for multiple emulsions stabilized by a single stimulable polymer, Soft Matter. 10 (2014) 7073–7087. https://doi.org/10.1039/C4SM00596A.
[41] H. Dupont, V. Héroguez, V. Schmitt, Elaboration of capsules from Pickering double emulsion polymerization stabilized solely by cellulose nanocrystals, Carbohydr. Polym. 279 (2022) 118997. https://doi.org/10.1016/j.carbpol.2021.118997.
[42] E. Rocca, J. Steinmetz, Inhibition of lead corrosion with saturated linear aliphatic chain monocarboxylates of sodium, Corros. Sci. 43 (2001) 891–902. https://doi.org/10.1016/S0010-938X(00)00115-3.
[43] S. Ghosh, D. Rousseau, Fat crystals and water-in-oil emulsion stability, Curr. Opin. Colloid Interface Sci. 16 (2011) 421–431. https://doi.org/10.1016/j.cocis.2011.06.006.
[44] Y. Chevalier, M.-A. Bolzinger, Emulsions stabilized with solid nanoparticles: Pickering emulsions, Colloids Surf. Physicochem. Eng. Asp. 439 (2013) 23–34. https://doi.org/10.1016/j.colsurfa.2013.02.054.
[45] L. Laporte, Propriétés des huiles utilisées en peinture : Rôle des siccatifs au plomb, fig. 3.40, p.131, Sorbonne-Université, 2022.
[46] J. Salvant Plisson, L. de Viguerie, L. Tahroucht, M. Menu, G. Ducouret, Rheology of white paints: How Van Gogh achieved his famous impasto, Colloids Surf. Physicochem. Eng. Asp. 458 (2014) 134–141. https://doi.org/10.1016/j.colsurfa.2014.02.055.
[47] V.D. Kiosseoglou, P. Sherman, Influence of Egg Yolk Lipoproteins on the Rheology and Stability of O/W Emulsions and Mayonnaise 1. Viscoelasticity of Groundnut Oil-in-Water Emulsions and Mayonnaise, J. Texture Stud. 14 (1983) 397–417. https://doi.org/10.1111/j.1745-4603.1983.tb00358.x.
[48] K. Maruyama, T. Sakashita, Y. Hagura, K. Suzuki, Relationship between Rheology, Particle Size and Texture of Mayonnaise, Food Sci. Technol. Res. 13 (2007) 1–6. https://doi.org/10.3136/fstr.13.1.
[49] L. de Viguerie, G. Ducouret, F. Lequeux, T. Moutard-Martin, P. Walter, Historical evolution of oil painting media: A rheological study, Comptes Rendus Phys. 10 (2009) 612–621. https://doi.org/10.1016/j.crhy.2009.08.006.
[50] T.G. Mason, New fundamental concepts in emulsion rheology, Curr. Opin. Colloid Interface Sci. 4 (1999) 231–238. https://doi.org/10.1016/S1359-0294(99)00035-7.

[51] R. Pal, Shear Viscosity Behavior of Emulsions of Two Immiscible Liquids, J. Colloid Interface Sci. 225 (2000) 359–366. https://doi.org/10.1006/jcis.2000.6776.
[52] S.R. Derkach, Rheology of emulsions, Adv. Colloid Interface Sci. 151 (2009) 1–23. https://doi.org/10.1016/j.cis.2009.07.001.
[53] M. Dinkgreve, J. Paredes, M.M. Denn, D. Bonn, On different ways of measuring “the” yield stress, J. Non-Newton. Fluid Mech. 238 (2016) 233–241. https://doi.org/10.1016/j.jnnfm.2016.11.001.
[54] J.D.J. van den Berg, Analytical chemical studies on traditional linseed oil paints, Universiteit van Amsterdam, 2002.
[55] J. van der Weerd, A. van Loon, J.J. Boon, FTIR Studies of the Effects of Pigments on the Aging of Oil, Stud. Conserv. 50 (2005) 3–22. https://doi.org/10.1179/sic.2005.50.1.3.
[56] L. de Viguerie, P.A. Payard, E. Portero, Ph. Walter, M. Cotte, The drying of linseed oil investigated by Fourier transform infrared spectroscopy: Historical recipes and influence of lead compounds, Prog. Org. Coat. 93 (2016) 46–60. https://doi.org/10.1016/j.porgcoat.2015.12.010.
[57] F. Busse, C. Rehorn, M. Küppers, N. Ruiz, H. Stege, B. Blümich, NMR relaxometry of oil paint binders, Magn. Reson. Chem. 58 (2020) 830–839. https://doi.org/10.1002/mrc.5020.
[58] C. Nimalaratne, J. Wu, Hen Egg as an Antioxidant Food Commodity: A Review, Nutrients. 7 (2015) 8274–8293. https://doi.org/10.3390/nu7105394.

Supplementary

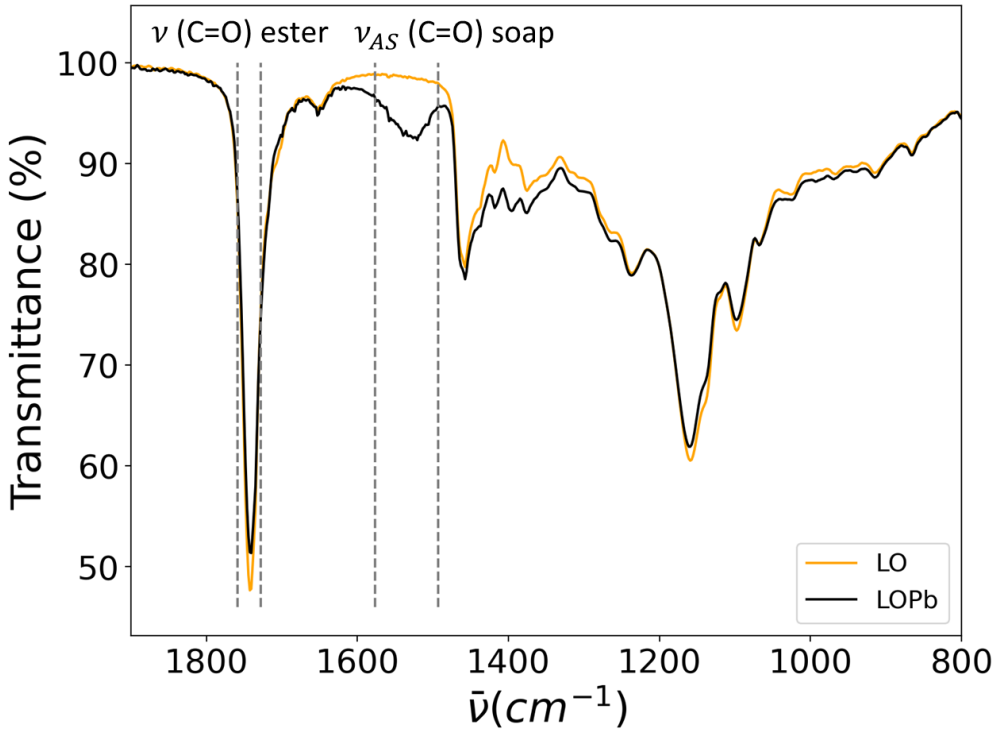

Figure S1: FTIR-ATR spectra of uncooked linseed oil LO (yellow) and lead-heated oil LOPb (black). The dashed lines indicate the regions used to compute the saponification rate, following the protocol proposed by Cotte [25].

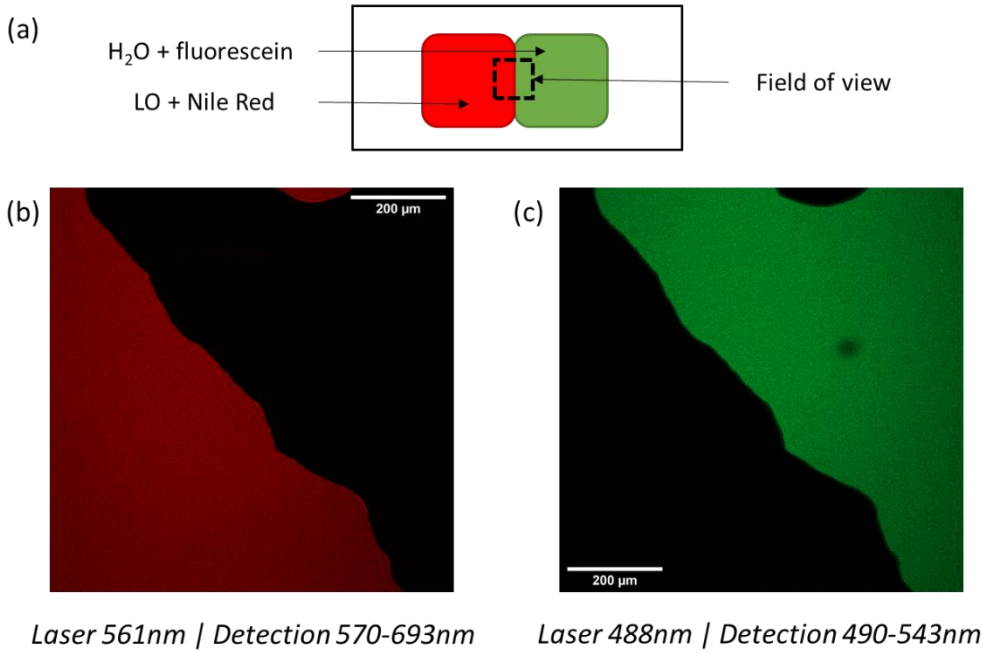

Figure S2: Strategy used for confocal microscopy imaging: (a) schematic representation of the sample used to tune the conditions of observation. (b) Imaging of the Nile Red. (c) Imaging of the fluorescein

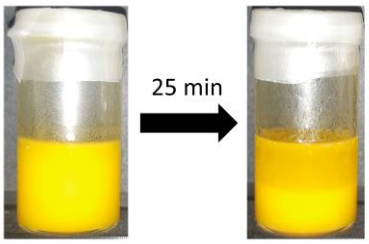

Figure S3: Photographs of an emulsion with 50wt% LO, prepared by a brief manual shaking of the vial, (left) right after emulsification, (right) 25 min later.

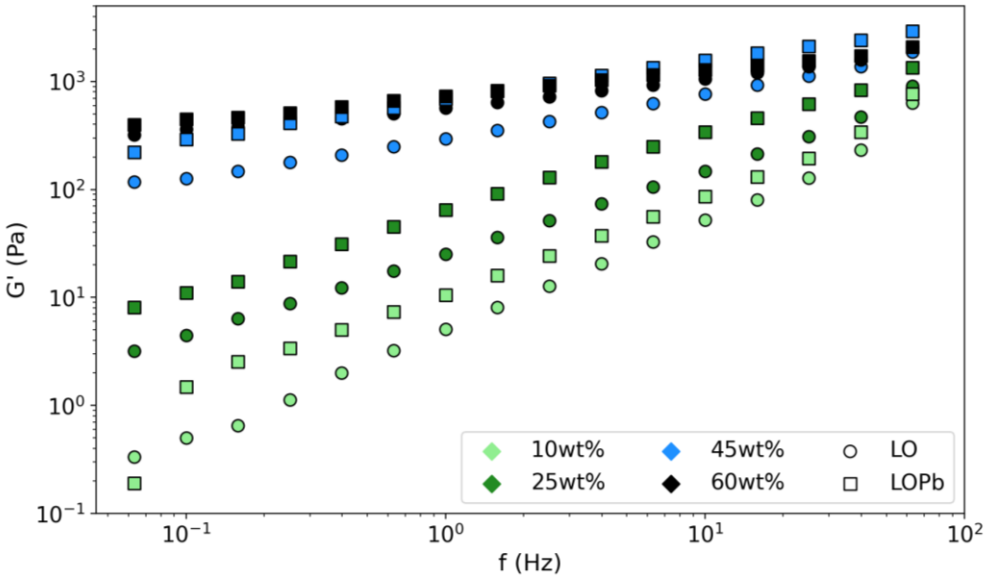

Figure S4: Frequency sweep measurements on o/w emulsions prepared with uncooked linseed oil LO (circles) or lead-heated linseed oil LOPb (squares), with various oil fractions. For the sake of clarity, only G' values are reported.

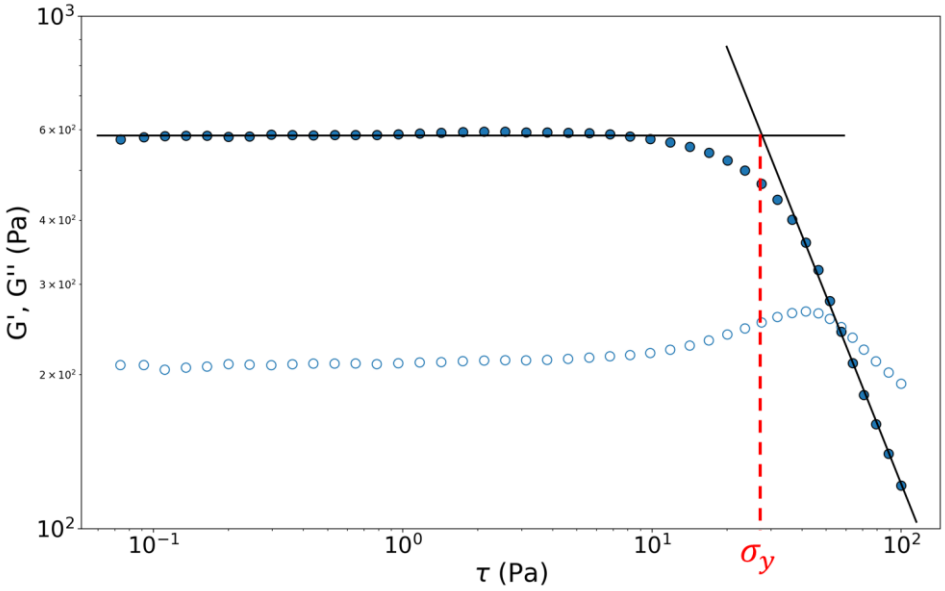

Figure S5: Yield-stress measurement: strain sweep experiment on an o/w emulsion with $\phi = 60wt\%$ LO. The yield stress is defined by the intersection of the horizontal line representing the behavior of G' (closed circles) in the linear viscoelastic region well below the yielding point, with the power-law equation representing the behavior of G' well above the yielding point.

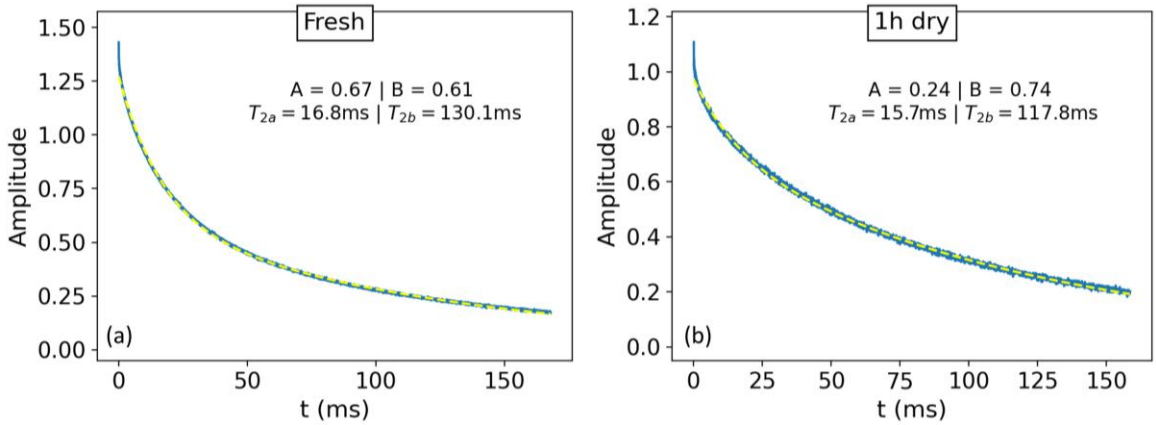

Figure S6 : Blue lines : relaxation of transverse magnetization of (a) a fresh emulsion with $\phi = 40wt\%$ LOPb, (b) a 250µm thick film of this emulsion after 1h of drying. Yellow dashed line : biexponential fit: $Ae^{-t/T_{2a}} + Be^{-t/T_{2b}}$. The strong decrease of the amplitude A of the component T_{2a}~$16ms$ can be attributed to water evaporation.